1. AGENCY USE ONLY (Leave blank)	2. REPORT DATE	3. REPORT TYPE AND DATES COVERED
	26 January 1998	Final

4. TITLE AND SUBTITLE
High Frequency Investigations of Lateral Superlattice Structures

5. FUNDING NUMBERS
DAAH04-95-1-0603

6. AUTHOR(S)
M Pepper

7. PERFORMING ORGANIZATION NAME(S) AND ADDRESS(ES)
Cavendish Laboratory
University of Cambridge
Madingley Road
Cambridge
CB3 0HE United Kingdom

8. PERFORMING ORGANIZATION REPORT NUMBER
Final

9. SPONSORING/MONITORING AGENCY NAME(S) AND ADDRESS(ES)
U. S. Army Research Office
P. O. Box 12211
Research Triangle Park, NC 27709-2211

10. SPONSORING/MONITORING AGENCY REPORT NUMBER
ARO 34601.1-PH

11. SUPPLEMENTARY NOTES
The view, opinions and/or findings contained in this report are those of the author(s) and should not be construed as an official Department of the Army position, policy, or decision, unless so designated by other documentation.

12a. DISTRIBUTION/AVAILABILITY STATEMENT
Approved for public release; distribution unlimited.

12b. DISTRIBUTION CODE

13. ABSTRACT *(Maximum 200 words)*
A description is given of work on the controlled movement of single electrons induced by a Surface Acoustic Wave in GaAs heterostructures and the formation of mini-gaps induced by a potential from patterned gates.

19980521 074

14. SUBJECT TERMS

15. NUMBER OF PAGES
10

16. PRICE CODE

17. SECURITY CLASSIFICATION OF REPORT	18. SECURITY CLASSIFICATION	19. SECURITY CLASSIFICATION OF ABSTRACT	20. LIMITATION OF ABSTRACT
UNCLASSIFIED	UNCLASSIFIED	UNCLASSIFIED	UL

Final Report

High Frequency Investigations of Lateral Superlattice Structures

1. Introduction

In a crystal, the periodic potential of the atomic lattices opens energy gaps of zero density electronic states. An electron with energy in a gap is Bragg reflected and hence cannot propagate through the crystal. Esaki and Tsu suggested that by defining a periodic potential longer than that of the atomic lattice it should be possible to observe Bragg reflections of transport electrons, giving rise to negative differential resistance (NDR). NDR was indeed observed subsequently in a three-dimensional semiconductor superlattice composed of alternating layers of AlGaAs and GaAs. The two-dimensional (2D) equivalent of such a device can be realised by patterning a lateral surface superlattice gate above a 2D electron gas formed at the interface of GaAs/AlGaAs heterostructure.

The aim of this research programme is to fabricate 2D lateral surface superlattices using high-resolution electron beam lithography. Unique physical phenomena, such as Bloch oscillations and miniband formation, have been predicted to be observable in a lateral superlattice. Most importantly, high frequency investigations of such a system can lead to high-precision determination of the change of this current, one of the most important physical quantities in solid state Physics. The ability to control bandstructure could lead to new types of device which could link up with single electron device research. Several samples have been supplied to Dr. B. Guenther at ARO and Duke University for optical measurements.

2. Double Cell Lateral Superlattice

Lateral one-dimensional surface superlattice with two unit cells have been fabricated with a pitch of 0.2 μm. At millikelvin temperatures, where electrons preserve phase coherence along the conduction channel, signatures of the minigaps formation with the periodicity of the device are observed. Calculations of the transmission coefficient of a multi-celled superlattice have shown that the strength of the mini-gap is critically dependent on the uniformity of the superlattice unit cells. To compensate for lithographic imperfections, a device with two unit cells are needed with independently controllable gate fingers as the gate finger voltages may be adjusted to optimise the individual barrier heights.

3. High Frequency Single Electron Transport

A surface acoustic wave (SAW) has been combined with a one-dimensional channel formed by a split gate. This results in a device which functions as a current source, with the SAW pumping an integer number of electrons per cycle across the channel. the resultant value of the current given by **I=nef**, where **n** is an integer, **e** is the magnitude of the charge on the electron, and **f** is the applied SAW frequency. The measured value of the current is within 0.3% of the expected value, demonstrating the precision with which electrons can be manipulated in this way.

This is clearly relevant to the construction of a quantized current standard, a longstanding metrological goal. The existing standards of voltage (based on the Josephson effect) and resistance (based on the quantum Hall effect) define the quantities in terms of the fundamental physical quantities of the Planck constant **h** and the charge on the electron **e**. If a current standard is also possible, then this would "close the metrological triangle" of electrical quantities.

The SAW devices bear a number of similarities to the most common approach to the problem, the electron turnstile. In this device, split gate barriers are drawn by electron-beam lithography to define an isolated quantum dot. The Coulomb blockade effect caused by the very small capacitance of the dot means that the number of electrons on the dot is well defined. The entrance and exit barriers are alternately raised and lowered to allow one electron at a time to tunnel through the device.

This approach has been extended in the charge pump, which has a series of quantum dots in a line. The barriers are lowered successively, allowing one electron through at a time in a "soliton" mode. These devices are relatively slow, however, operating in the MHz range.

The SAW devices offer higher operation speeds. A (mechanical) SAW moving on a piezoelectric surface such as GaAs has an accompanying spatially varying electrostatic field. Electrons are trapped in the potential minima associated with the SAW, and carried along. They are then passed across a split gate. The combination of longitudinal confinement by the SAW potential and lateral confinement by the split gate produces a dot. As with the electron turnstile, Coulomb blockade operates, restricting the number of electrons which can occupy this dot. The crucial difference is that the SAW potential moves across the split gate with the mechanical wave, and carries the electrons across itself.

This different type of operation permits the use of a higher range of frequencies. To obtain good longitudinal confinement by the SAW, wavelengths in the range of 1μm and below are required. On GaAs at low temperatures, this gives an operation frequency of around 2.7GHz, three orders of magnitude higher than the electron turnstiles. The resulting current assuming one electron is transferred across the split gate per cycle is about 400pA.

Several devices have been fabricated which show the signature of quantized charge transport. The acoustoelectric current is measured as the split gate is pinched off (driven below the last conductance plateau). Under the correct experimental conditions a series of steps are observed, with heights at the current corresponding to transfer of an integer number of electrons per cycle.

As the voltage applied to the split gate is made less negative, the SAW potential superimposes on the saddle point to form a local minimum. This carries electrons across the gate as it moves. As the minimum widens, first one, then two, **etc.** electrons are carried across in each cycle.

The most obvious feature of the results in figures 1 and 2 is that the quantized current steps are not visible at all power levels. As the power is raised, then at first only one step is seen. There is then a region where the

current is not flat, which then develops into the next step. This is believed to be a region where the occupation probability of the highest electron energy level in the dot is finite, but not unity. Naturally, when the occupation probability is one, then all the dots will be occupied, giving the step in the observed current. If the probability falls below one, for example if there is a finite probability of the upper electron tunnelling out of the dot, then the current will vary with gate voltage.

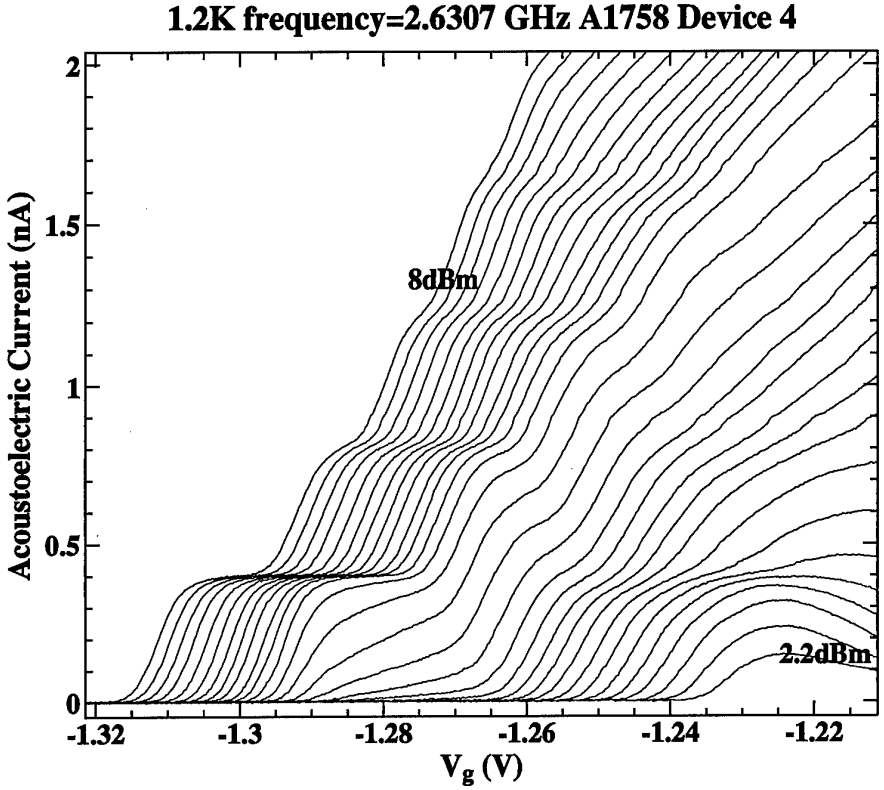

Figure 1. Acoustoelectric current vs. gate voltage at different SAW power levels for device A1758D. The steps in current corresponding to transfer of an integer number of electrons are clearly visible. Note the range of power levels where the steps do not appear. This region is believed to occur when the occupation probability of the highest electron energy level is between 0 and 1.

The result in figure 2 appears to be much noisier than that shown in figure 1, displaying large irreproducible fluctuations in the current. Further measurement showed these fluctuations to be time dependent. The origin is believed to be similar to the Random Telegraph Signals (RTSs) first observed in silicon MOSFETs. A single electron trap state dominates the channel conductance. When the occupation of the state changes, then the shape of the channel alters. Since the quantized charge transport is a relatively sensitive effect, the measured current changes. Since it is not visible in the results in figure 1, we believe that this effect can be minimised by careful choice of material.

The most important question concerns the accuracy of the quantized current. All devices which have demonstrated this effect have delivered a current accurate to within 1%. The most accurate result, from device A1758D, is shown in figure 3. This shows that, although the step is in the correct position, it is not flat. There is a visible slope, of approximately $0.2\%mV^{-1}$. Since all devices had similar split gate geometry, one would expect them all to display a similar degree of accuracy. Nevertheless, the devices display a remarkable degree of accuracy for such a conceptually simple device.

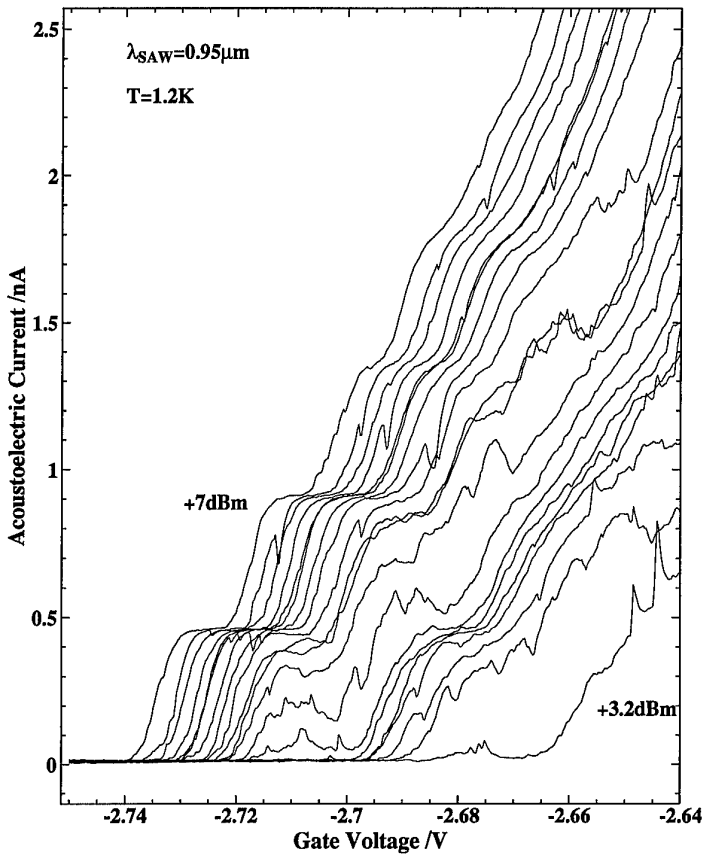

Figure 2. Quantized current steps shown by device A1470H. Note the large irreproducible fluctuations, particularly in the region where the steps are not visible. These are believed to be due to Random Telegraph Signal fluctuations, as mentioned in the text.

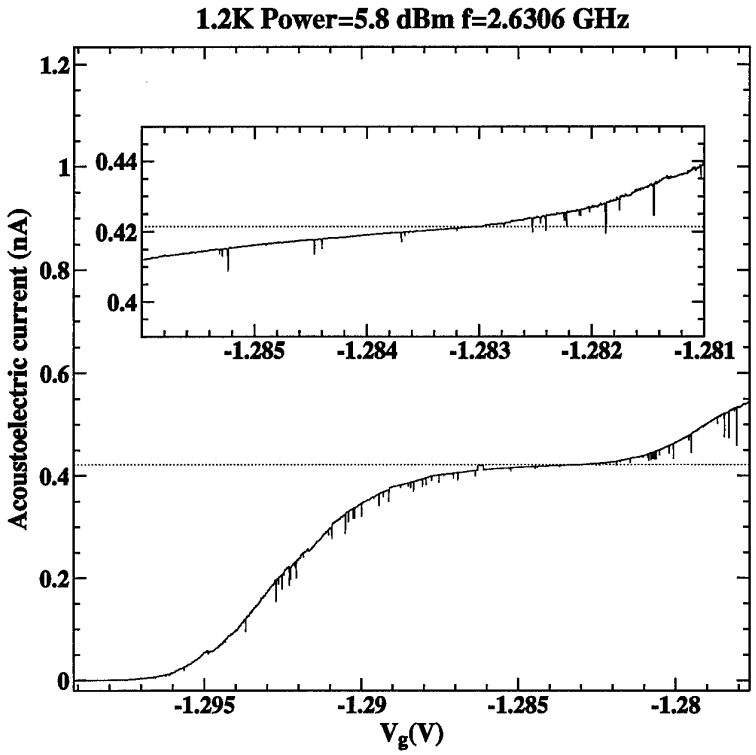

Figure 3. Accurate data of current step on device A1758D. The RTS noise is much lower than A1470H, but data reveals that the step is not completely flat. Inset shows magnification of step region. Slope is approximately 0.2%mV^{-1}. Dotted line shows value ef. T=1.2K, f=2.6306GHz, P_{SAW}=5.8dBm.

4. T-shaped Stub Tuner

It has been proposed that a ballistic electronic analogue of a microwave stub-tuner could prove to be a feasible realisation of a transistor based on quantum mechanical principles. It has been calculated that a small change in the transverse arm length should lead to a large change in the quantum-mechanical transmission coefficient and hence in the device conductance. Even allowing for thermal smearing, some of the predicted structure in conductance is observable at finite temperatures. The practical problem is that it is difficult to maintain electron phase coherence through a device. Therefore it is desirable to make the conduction channel as short as possible. We have fabricated T-shaped channels where the source-drain distance for the active region is 250 nm, much smaller than the micron-scaled devices reported in the literature. Low-temperature measurements were made on devices with a stub length of 100 nm. We have observed replicated conductance dips superimposed on two quantised ballistic conductance steps as shown in figure 4, convincing experimental evidence for phase-coherent length resonance effects. The fact that those resonant features are reproducible at two different cooldowns demonstrates that impurity scattering is negligible in our system.

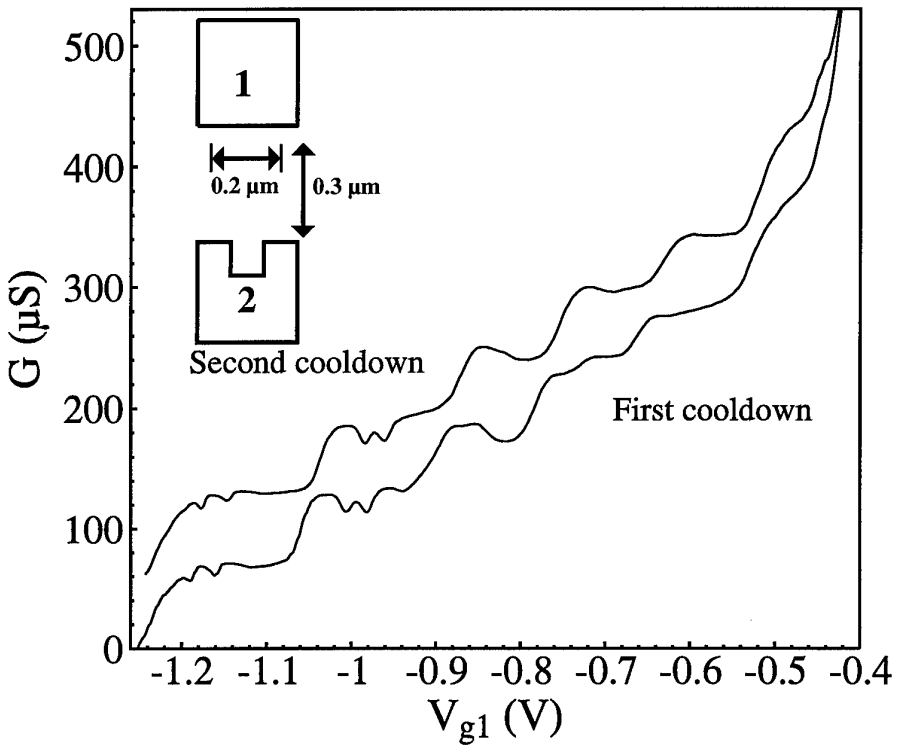

Figure 4. Lower curve: conductance measurements as a function of gate voltage $G(V_{g1})$ for V_{g2} = -1.4 V in the first cooldown. Higher curve (offset by 50 μS): $G(V_{g1})$ for V_{g2} = -1.72 V in the second cooldown. The inset shows the device geometry.

Figure 5 shows $G(V_{g1})$ for V_{g2} = -1.4 V at various magnetic field. The oscillations superimposed on ballistic conductance steps gradually disappeared as *B* is increased. The application of a perpendicular magnetic field breaks time reversal symmetry, suppressing coherent backscattering of electrons in the ballistic channel. This is analogous to suppression of weak localisation effects in diffusive transport by a perpendicular magnetic field.

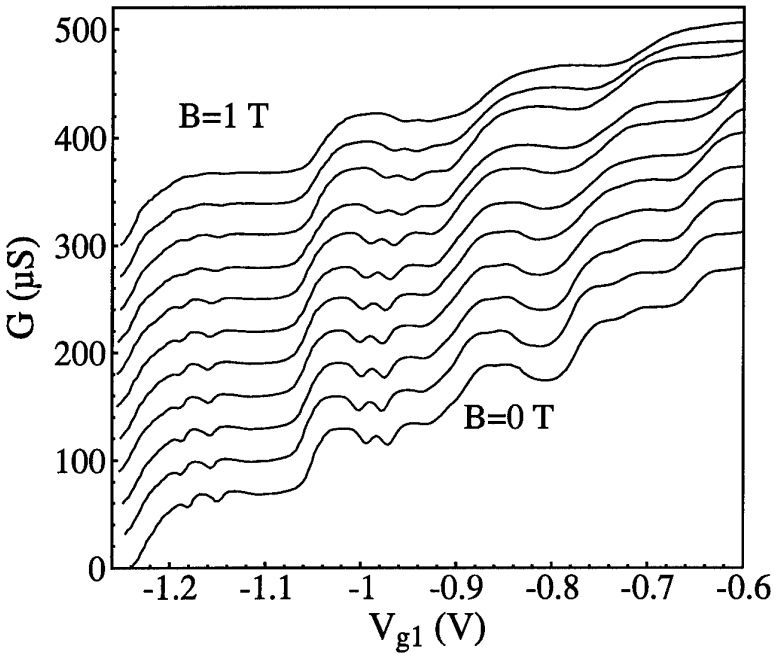

Figure 5. $G(V_{g1})$ at various magnetic fields B for for V_{g2} = -1.4 V. From bottom to top: B= 0 to 1 T in 0.1 T steps. Traces are successively offset by 30 μS for clarity.

As the temperature is increased, the conductance oscillations become weaker and we recover ballistic conductance steps as illustrated in figure 6. This effect is due to a reduction in phase coherent time at higher temperatures, leading to an enhancement of phase-breaking rate.

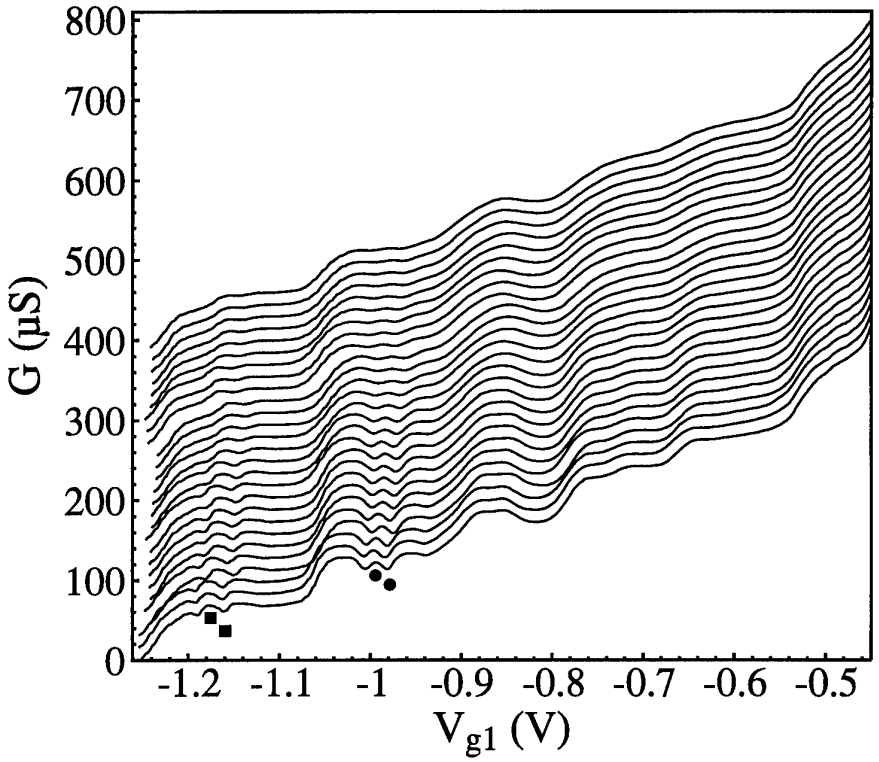

Figure 6. $G(V_{g1})$ at different temperatures T for V_{g2}=-1.4 V. From bottom to top: T =0.3 K to 1.5 K in 0.1 K steps and T=1.85 K to 3.25 K in 0.1 K steps. Traces are successively offset by 15 μS for clarity.

Provided that the amplitude of a peak and a trough in conductance oscillations *Amp* is given by

$$Amp \propto \exp(-\tau/\tau_\phi), \quad (1)$$

where τ and τ_ϕ are the traversal time for an electron to pass through the ballistic channel and electron phase coherent time, respectively. from this we know that

$$\ln(Amp) \propto -\tau/\tau_\phi + A, \quad (2)$$

where A is a constant. Here we assume that the traversal time τ is temperature independent which holds when the thermal broadening is much smaller than the Fermi energy in our system. From the amplitude of the conductance oscillations at various temperatures we have

$$\ln(Amp(T)) \propto -1/\tau_\phi + A/\tau, \quad (3)$$

Figure 7 shows the normalised logarithm of the conductance oscillations amplitude at various temperatures. From the fit we obtain $1/\tau_\phi = 0.2147T + 0.0717T^2\ln T$. The linear term in T arises from one-dimensional electron scattering whereas the $T^2\ln T$ term corresponds to the well-known Landau-Baber scattering in two dimensions. Thus we conclude that in our system two-dimensional scattering occurs in the wide regions of the channel where there are many subbands occupied, whereas one-dimensional electron scattering takes place around two barriers, the narrow regions of the channel where only one or two subbands are occupied. Our seminal results provide a good understanding for a single T-shaped channel, the unit cell of a finite T-dot array where Bragg reflections are predicted to be observable.

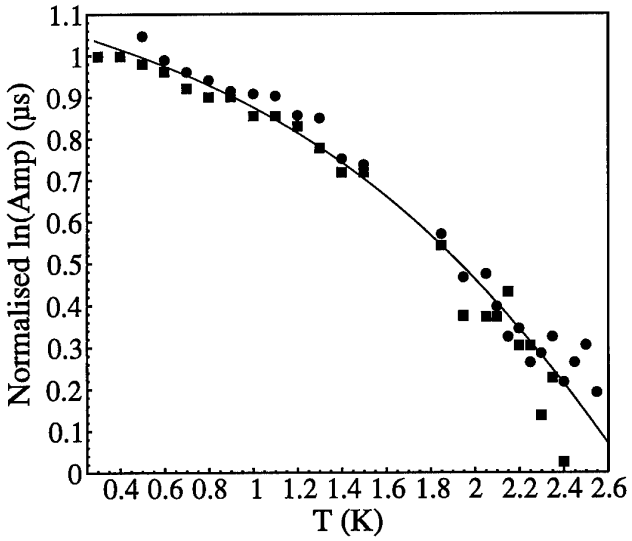

Figure 7. Normalised logarithm of the amplitude *Amp* of the conductance oscillations on the first conductance plateau step (marked by squares) and on the second step (marked by circles) at various temperatures *T*. The solid line shows a fit $\ln(Amp(T)) = -1.09 - 0.2147T - 0.0717T^2\ln T$.

5. Clean one-dimensional Channel with Two Independent Tunable Barriers

We have recently developed a technique utilising crosslinked PMMA as an insulating layer. Using this method, we have fabricated a device comprised of a split-gate structure with two gate fingers on top, separated by a layer of crosslinked PMMA, as shown in figure 8.

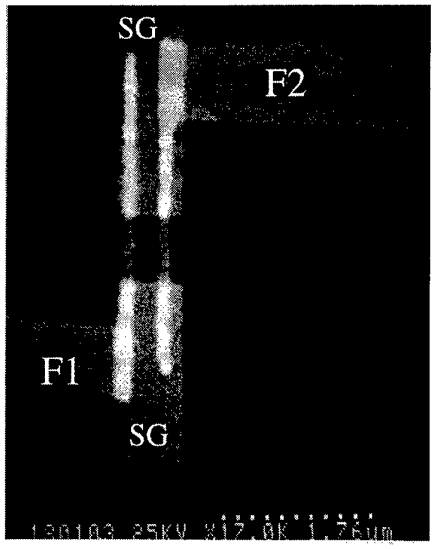

Figure 8. An SEM micrograph of a split-gate sample (SG) and two tunable finger gates (F1 and F2), with a crosslinked PMMA layer in between.

Using such a versatile system, we have discovered interesting phenomena. First, by defining two tunnel barriers in such a clean one-dimensional channel, we observe pronounced Coulomb oscillations as a function of split-gate voltage. For loosely bounded Coulomb oscillations, we observe splitting of single electron tunnelling peak as the in-plane magnetic field is increased as shown in Figure 9. This is ascribed to a Zeeman effect.

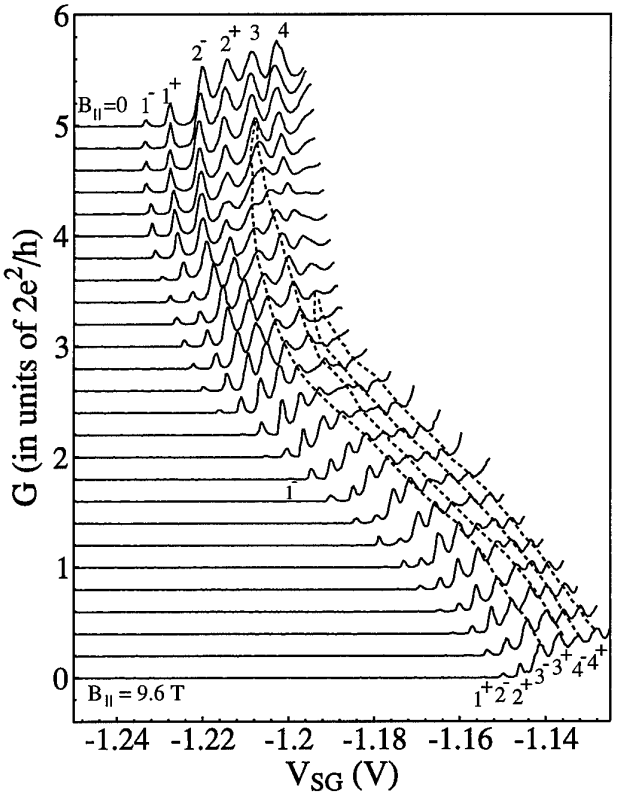

Figure 9. $G(V_{SG})$ for $V_{F1}=V_{F2}=-1.5$ V at various in-plane magnetic fields. From top to bottom: B= 0 to 9.6 T in 0.4 T steps. Curves are successively offset for clarity. Dashed lines serve as a guide to the eye, indicating splitting of peaks which are due to Zeeman effect.

Second, we also observe a transition from Coulomb charging in the presence of fully transmitted 1D channels, to conventional Coulomb charging when no 1D channels are transmitted through the quantum dot. This result has demonstrated the importance of Coulomb interactions between electrons even when the conductance through a quantum dot is greater than $2e^2/h$. The fully transmitted 1D channels only partially screen the Coulomb parts thus Coulomb charging can occur in the metallic regime. This effect, so called "metallic Coulomb charging" [4], has never been observed before in a mesoscopic system at zero magnetic field.

6. Quantum Molecule

The straight-forward extension of the work described in section 5 is a "quantum molecule" comprising a split-gate structure with three fingers on top, as shown in figure 10. This system provides a fertile testing ground for studying coupling between artificial atoms. The potential modulation along the ballistic channel can be varied by applying various voltages on F1, F2 and F3, independently. In additional to the formation of minibands, we are able to measure the potential profile along the ballistic channel by pinching-off the channel with different finger gate at one time. From the pinch-off characteristics and source-drain bias data, we are able to map out the potential modulation as a function of finger gate voltages, testing the well-known saddle-point model. Thus we can perform "scanning probe microscopy" along the ballistic channel which at present research workers are using AFM and STM. However, the presence of a high-density of surface states makes the investigations extremely difficult. Detailed studies of a "quantum molecule" will be performed at the Cavendish Laboratory at milli-kelvin temperature where the electron wave-nature is evident in the ballistic regime. Further studies on this system will be carried out at ARO by our collaborators.

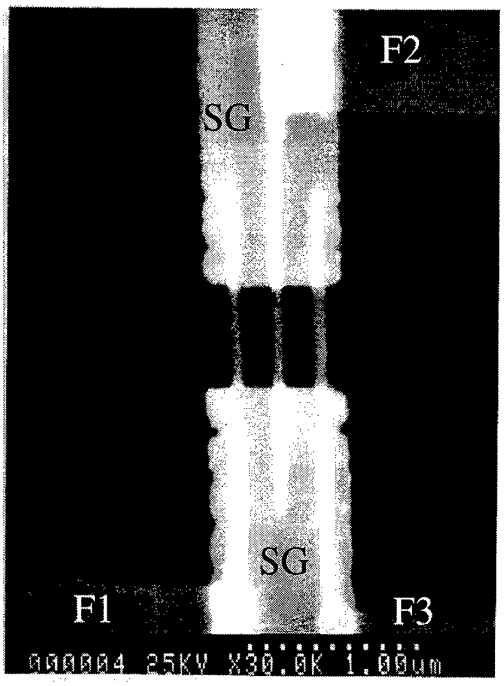

Figure 10. An SEM micrograph of a split-gate sample (SG) and three finger gates (F1, F2 and F3), with a crosslinked PMMA layer in between.

7. High-frequency Studies of T-shaped Quantum Dot Transistors-Collaboration with ARO

We have now extended our work on T-shaped ballistic channels described in section 4, in the high frequency front with T-shaped quantum dot with a bow-tie antenna. We have designed a new optical mask and such design allows good microwave amplification to avoid electron heating in the quantum dot. This is particularly important as the heating can smear out quantum-mechanical effects. By applying a small microwave signals on top of a dc voltage, we can investigate the microwave response of a T-shaped quantum dot transistor. The samples were fabricated on a specially designed ultra high-mobility GaAs/ AlGaAs heterojunction. The as-grown MBE parameters are summarised in the table as follows.

Matrix	Thickness	Doping
GaAs	100 A	-
AlGaAs	400 A	$7x10^{12}$
AlGaAs	700 A	-
GaAs	1 μm	-

Table 1. The MBE parameters of the GaAs/AlGaAs heterostructure for T-shaped dots.

By utilising the well-known persistent photoconductivity effect in AlGaAs, the two-dimensional electron gas has a carrier density of $4x10^{15}$ m^{-2} with a mobility of 200 m^2/Vs. The initial test of the T-shaped quantum dot samples shows three ballistic conductance steps at 4.2 K, demonstrating the extremely high-quality of our MBE material. Three samples have been shipped over to our ARO collaborator, Dr. Guenther in Duke University for detailed high-frequency studies, as yet no results have been forthcoming.

8. Publications Supported by the Grant

1. "High-frequency single-electron transport in a quasi-one-dimensional GaAs channel induced by surface acoustic waves"
J.M. Shilton, V.I. Talyantskii, M. Pepper, D.A. Ritchie, J.E.F. Frost, C.J.B. Ford, C.G. Smith and G.A.C. Jones, J. Phys. Cond. Matter 38, L531-L539 (1996).

2. "Single-electron transport in a one-dimensional channel by high-frequency surface acoustic waves"
V.I. Talyantskii, J.M. Shilton, M. Pepper, C.G. Smith, C.J.B. Ford, E.H. Linfield, D.A. Ritchie and G.A.C. Jones, Phys. Rev. B 56, 15180-15184 (1997).

3. "Experimental studies of T-shaped quantum dot transistors: phase-coherent electron transport"
C.-T. Liang, J.E.F. Frost, M. Pepper, D.A. Ritchie and G.A.C. Jones, Solid State Commun. 105, 109-111 (1998).

4. "Quantized current in a one-dimensional channel induced by surface acoustic waves"
V. I. Talyanskii, J. M. Shilton, J. Cunningham, M. Pepper, C. J. B. Ford, C. G. Smith, E. H. Linfield, D. A. Ritchie and G. A. C. Jones, to be published in Physica B (1998).

9. Personnel Associated with the Project

Dr. C.-T. Liang and Dr. J.M. Shilton.

10. Invention

There are no inventions.